

Technical paper

Analysis and Modeling of Boundary Layer Separation Method (BLSM)

Dóra Pethő,^{1,*} Géza Horváth,¹ János Liszi,² Imre Tóth¹ and Dávid Paor¹

¹ University of Pannonia, Institutional Department of Chemical Engineering Science, H-8201 Veszprém, Hungary

² University of Pannonia, Department of Physical Chemistry, H-8201 Veszprém, Hungary

* Corresponding author: E-mail: pethod@almos.uni-pannon.hu

Received: 19-12-2009

Abstract

Nowadays rules of environmental protection strictly regulate pollution material emission into environment. To keep the environmental protection laws recycling is one of the useful methods of waste material treatment. We have developed a new method for the treatment of industrial waste water and named it boundary layer separation method (BLSM). We apply the phenomena that ions can be enriched in the boundary layer of the electrically charged electrode surface compared to the bulk liquid phase. The main point of the method is that the boundary layer at correctly chosen movement velocity can be taken out of the waste water without being damaged, and the ion-enriched boundary layer can be recycled. Electrosorption is a surface phenomenon. It can be used with high efficiency in case of large electrochemically active surface of electrodes. During our research work two high surface area nickel electrodes have been prepared. The value of electrochemically active surface area of electrodes has been estimated. The existence of diffusion part of the double layer has been experimentally approved. The electrical double layer capacity has been determined. Ion transport by boundary layer separation has been introduced. Finally we have tried to estimate the relative significance of physical adsorption and electrosorption.

Keywords: Boundary layer, electrosorption, nickelized nickel electrode, porous nickel electrode, industrial alkaline waste water

1. Introduction

The development of industrial technologies is coupled with more and more waste emission waiting for treatment to protect the quality of environment and the natural resources. We must make efforts to apply wasteless production technologies or technologies with minimal waste emission.

There are more and more strict environmental protection rules for waste formation regulating e.g. metal and salt content, and quantity of other organic and inorganic materials of chemical factory waste water. To keep the laws gives the reason for modernization treatment of the incidentally formed waste materials, or if it is possible it's recycling.

We have developed a new method for the treatment of industrial waste water and named boundary layer separation method (BLSM). The main point of the method is that the formed ion enriched boundary layer of the electrically

charged electrode surface at correctly chosen movement velocity can be taken out of the waste water, and can be recycled. According to the new process the amount of ions are usable in another system or can be enriched to decrease toxic material emission.

The method is based on electrosorption phenomenon. Electrosorption is an adsorption on electrically charged electrode surface.¹ There are galvanostatic or potentiostatic methods of electric polarization². In practice mostly the galvanostatic method is favoured.²⁻⁴ Electrosorption of cations takes place on the cathodically polarized (negative) electrodes. Superposition of electrosorption and the physical adsorption (taking place on non-charged electrode) can be observed. In case of reversed direction of electrochemical polarization, desorption of cations is observed.⁵⁻⁸ Using this phenomenon ion transport with electrosorption can be realized.

During electrosorption electric double boundary layer is formed on the electrode solution interface. There

are two main parts of the electric double boundary layers: the Helmholtz-layer, and the diffusion layer. While moving the electrode the breakaway of diffusion layer can be experienced, then zeta-potential is formed between the static and moving parts.

Electrosorption is a surface phenomenon. The efficiency of the process is high if the electrode surface is large. Mostly porous carbon-electrodes with high specific area are used.^{1,3,9–14,31–33} High surface electrode can be made of metal, too. With hydrogen reduction of NiO, Co₃O₄ and Fe₂O₃ macroporous Ni, Co and Fe can be produced.¹⁵ Porous Ni, Cu, Ag, Pt, and Au can be produced by precipitation of metal to colloid silicic acid, then after calcinations silicon dioxide is removed by HF.¹⁶ Among electrochemical methods production of platinised platinum is widely known. Similarly high surface “black” or “gray” nickel electrode can be produced as well.^{17–19} Large surface is not always a definite advantage, namely if pore size distribution is not appropriate because of size exclusion, a certain part of the surface electrochemically does not work.

By electrosorption inorganic ions²⁴ and organic ions e.g. phenols,¹⁰ pyridine,² aniline and bipyridines,³ thiocyanates¹ can be removed from aqueous solutions. Examples for colloid particle removal also can be found.²¹ Among practical applications waste water purification,^{2,3,10,19,20} and water desalination^{22–29} are respectful processes. The invented process we named BLSM is a novelty from technical point of view.

2. Experimental

2.1. Preparation of Nickelized Nickel Electrodes

Nickel was precipitated onto the nickel plate by electrolysis. Nickel plate surface treatment before electrolysis was carried out in different steps, as follows: first mechanical polishing, then degreasing with 10 mol dm⁻³ sodium hydroxide water solution, washing with ion exchanged water, drying, leaching in chloroform or carbon tetrachloride, finally acid etching in 30% (m/m) hydrochloric acid in water at boiling temperature. After pre-treatment electrolyte solution proposed by Berezina and co-workers¹⁷ was applied. The electrolyte contained 33 g dm⁻³ NiSO₄, 33 g dm⁻³ (NH₄)₂SO₄ and 14 g dm⁻³ K-Na-tartrate in water, and the pH of the solution was 5.1. According to our experiences no uniform and stable nickel coating could be achieved with the above solution. We have observed that properties of nickel coating precipitated during electrolysis depended strongly on solution pH. Bright shining grey coating was formed at pH = 7.0 while black pitted coating at pH = 8.0. The pH was increased by adding NH₄OH in water solution. At pH = 7.5 value opalescent solution was formed resulted by Ni(OH)₂ precipi-

tation. Precipitate could be dissolved with EDTA (ethylenediaminetetraacetic acid) into a complex form. The solution had deep blue color in pH = 9.5–10.0 range from which uniform, black and stable coating could be precipitated. Current density of electrolysis had to be smaller than 0.1 Amper cm⁻². During electrolysis solution pH could change causing surface quality weakening. Constant pH value could be assured by the properly large amount of solution, or by adding NH₄OH in water.

2.2. Preparation of Porous Nickel Electrodes

Porous electrodes were prepared by this method as porosity assured larger surface area. The starting powder mixture contained Raney-nickel (Merck) glowed at 60 °C temperature in 90–93% (m/m), silver chloride (Merck) in 2–5% (m/m) silver concentration, and paraffin in 5 % (m/m) amount. Paraffin was pre-treated to get the proper homogeneity and porosity as follows: Paraffin was melted in warm (70 °C temperature) water and beside strong mixing surface active material (washing-up detergent) was added. The formed emulsion was rapidly cooled down on ice cube packing, and then paraffin particles were dried at room temperature. The powder mixture was compressed in steel ring by hydraulic press with 6–8 metric tonnes to form cylindrical pastilles D = 10 mm diameter and 2 mm thickness. Pastilles were heat treated followed by reduction.

There were two steps of heat treatment. First all organic materials were burnt out in oxidative atmosphere. Heating-up rate was about 200 °C h⁻¹. Reaching 400–450 °C pastilles were kept at this temperature for 30 minutes. The solid paraffin first melted, and then converted to gas phase by cracking. If the heating-up rate was higher than the above mentioned, the formed cracking gases could destroy pastilles.

In the second step pastilles were kept for 30 minutes in inert (nitrogen) atmosphere at 960–1100 °C temperature. Then was formed the nickel silver alloy, which increased electrical conductivity and improved the mechanical properties of the electrode. In case of the first step omission splits were formed on the porous electrode surface and it became useless.

Reduction was carried out in flowing hydrogen atmosphere at 550 °C temperature. The end of reduction was indicated by the very low water content of the reactor outlet gas (2.67 kPa partial pressure of water).

2.3. Experimental Setup

Laboratory scale experimental equipment and peripheral instruments are presented in Figure 1.

Basic regulation was done by process controlling computer, where polarization potential could be adjusted. Electrosorption-desorption process was indicated by cur-

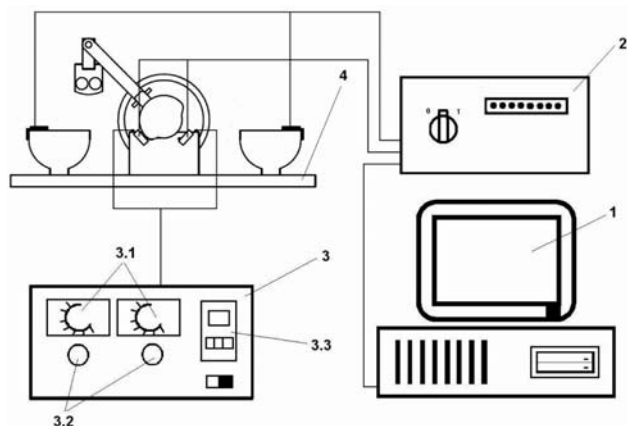


Figure 1. Experimental equipment and peripheral instruments

1. Process controlling computer, 2. Power supply, 3. Controlling unit, 3.1. Adjustable timers, 3.2. Control lamps, 3.3. Programmable cycle counter, 4. Automatic electrosorption equipment

rent intensity changes, so intensity of current flowing across the cells were continuously measured and registered. Power supply joined to the computer providing the necessary polarization potential. Adsorption and desorption times could be exactly adjusted by the adjustable timer of the controlling unit. The present condition of adsorption-desorption processes was indicated by the control lamps. Required cycle number could be adjusted by the programmable cycle counter.

The main part of the system is the automatic electrosorption equipment. Structure and units of equipment are presented by Figure 2.

The mobile working electrodes are fixed to a driven axle being lifted by the moving lever from the anode-space vessel to the cathode-space vessel. Moving lever is moved by a driven axle having at one end a programme regulation disc with fitting four micro switchers. These micro

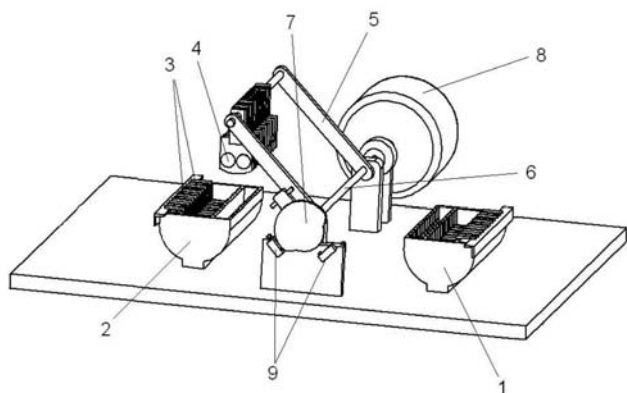


Figure 2. Automatic electrosorption equipment

1. Anode-space vessel, 2. Cathode-space vessel, 3. Graphite counter electrodes, 4. Mobile working electrodes, 5. Moving lever, 6. Driven axle, 7. Programme regulation disc, 8. Electric motor, 9. Micro switchers

switchers assure the stoppage of moving lever in given position, the switching on and off the polarization potential, and the electric pole change. An electric motor joins to the other end of the driven axle through transmission rolling the driven axle. There are graphite counter electrodes fixed in the vessels. Mobile working electrodes are placed among them.

The experimental equipment was stable, reliable in operation, could be easily handled, and the electrochemical parameters could be varied quickly and in wide range. During the measurement $0.05 \text{ mol dm}^{-3} \text{ NaOH}$ (Fluka) in water solution was used.

3. Results and Discussion

3.1. Electrochemically Active Surface Area

Electrolytic double boundary layer was formed on the electrode-solution interface having two main parts as the ion concentration dependent Helmholtz-layer, and the ion concentration independent diffusion layer. The electrolytic double boundary layer could be considered to be capacitor. When electric current had flown through ideal polarized electrode, than there was no transfer of electric charge, and electric current changes only charge of capacitor.

$$\frac{dQ}{d\varepsilon} = \frac{Idt}{d\varepsilon} = C_t \quad (1)$$

where Q means charge, ε capacitor potential, I electric current density, t time, and C_t the polarization capacity at t given time. C_t means at $t = 0$ time the capacity of boundary double layer in case of partial polarization.

Examined electrode potential compared to the saturated calomel electrode potential ($\Delta\varepsilon = \varepsilon - \varepsilon_{\text{calomel}}$) was measured in function of time beside constant electric current density.

Initial tangent ($t = 0$) of $\Delta\varepsilon$ versus t curve ($t = 0$):

$$\text{tg}\alpha = \frac{d(\Delta\varepsilon)}{dt} = \frac{d\varepsilon}{dt} \quad (2)$$

Polarization capacity from equations (1) and (2):

$$C_t = \frac{Idt}{d(\Delta\varepsilon)} = \frac{I}{\text{tg}\alpha} \quad (3)$$

Assuming flat capacitor $C_t = \varepsilon_0 A/d$, where ε_0 is vacuum permittivity, A surface, d distance between conductors (insulator thickness). The result on the basis of equation (3):

$$\frac{\varepsilon_0 A}{d} = \frac{I}{\text{tg}\alpha} \quad (4)$$

If electrochemically active surfaces of the two different electrodes are compared to each other within the sa-

me conditions of measurements, then the next equation can be used:

$$\frac{A_1}{A_2} = \frac{\operatorname{tg}\alpha_2}{\operatorname{tg}\alpha_1} \quad (5)$$

where 1 and 2 indexes mean different electrodes.

High surface area electrodes were compared to the smooth surface (polished) nickel electrode surface based on the above simple considerations at constant electric current $I = 10$ mA, solution concentration 0.05 mol NaOH/dm³ water, distance between electrodes 10 mm. If the electrochemically active surface of the smooth surface (polished) nickel electrode was considered theoretically 1 unit, than that of nickelized nickel electrode 50 unit, and that of the porous nickel electrode 214 unit. These data agreed with special literature data (measured by other methods) for copperized copper,^{4,30} and nickelized nickel.¹⁸

3. 2. Double Layer Capacity

F. Béquin and co-workers examined the electrosorption of lithium on active carbons.¹¹ Electrochemical cell modeling with simplified electric model is shown on Figure 3, where R_e is resistance of electrolyte solution, R_t is electric charge transfer resistance, C_d means double layer capacity.

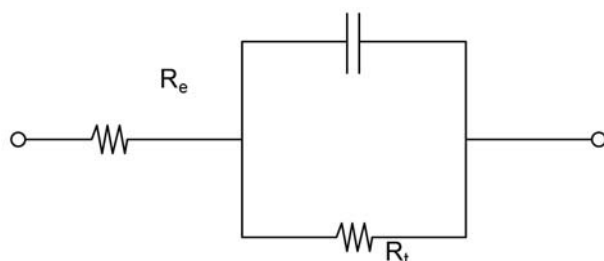


Figure 3. Simplified electric model of electrochemical cell

F. Béquin and his co-workers have proved, that U potential difference of electrochemical cell changing in time between electrodes beside constant I current stream in cell is:

$$U = R_e I + R_t I - R_t I e^{-\frac{t}{R_t C_d}} \quad (6)$$

If $t = 0$, then according to equation (6)

$$U_{(t=0)} = R_e I \quad (7)$$

R_e value comes from equation (7), if $t \rightarrow \infty$

$$U_{(t=\infty)} = (R_e + R_t) I \quad (8)$$

R_t can be determined from equation (8). The derivative of potential in time beside constant I :

$$\left. \frac{dU}{dt} \right|_{t=0} = \frac{I}{C_d} e^{-\frac{t}{R_t C_d}} \quad (9)$$

If $t = 0$, then from equation (9)

$$\left. \frac{dU}{dt} \right|_{t=0} = \frac{I}{C_d} \quad (10)$$

By equation (10) from the initial tangent of U versus t curve electric layer capacity C_d can be calculated.

We carried out the experiments with solution concentration 0.05 mol NaOH/dm³ water beside $I = 10$ mA constant electric current. Figure 4 shows the potential difference U in Volts versus time in seconds for the two different electrodes. Electrical charge of electrodes could be determined by capacity C_d and potential difference U between electrodes: $Q = C_d U$. Knowing Q electric charge sodium ion quantity taken up by electrosorption could be calculated by Faraday law. Related to 1 m² electrode geometrical surface in case of nickelized nickel electrode the taken up sodium mass was 298 mg Na⁺, while for porous nickel electrode it was 127 mg Na⁺. Based on equations (7) and (8) the electrochemical cell parameters could be determined. Parameters for nickelized nickel electrode: $R_e = 122 \Omega$, $R_t = 125 \Omega$, $C_d = 0.29$ F; for porous nickel electrode: $R_e = 62 \Omega$, $R_t = 108 \Omega$, $C_d = 5$ F.

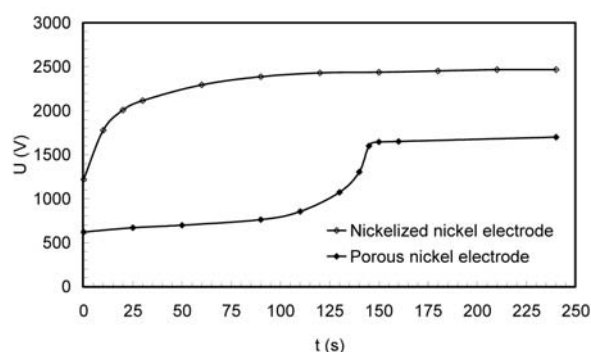


Figure 4. Potential difference in function of time at $I = 0.01$ A

3. 3. Diffuse Part of the Electrochemical Double Layer

In case of relative movement of electrode and solution the diffuse part breakaway of the electrochemical double layer happened and zeta-potential came into being. The value of zeta-potential depended on the movement velocity. Additionally the place of double layer breakaway influenced the efficiency of ion transfer as well. The more part of double layer was transferred from one solution to the other, the more effective the ion transport was. It was practical to examine the changes of the zeta potential (thus the place of double layer breakaway) with relative velocity within the actual system. Zeta potential was measured by the equipment presented in Figure 5.

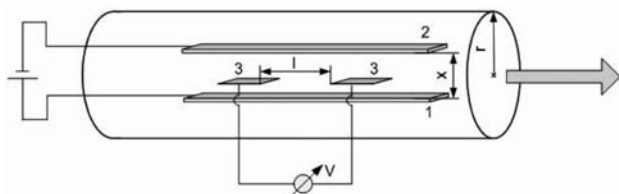


Figure 5. Measurement of zeta potential

$r = 15 \text{ mm}$, $x = 15 \text{ mm}$, $l = 40 \text{ mm}$, 1. Cathode, 2. Anode, 3. Auxiliary electrode

In the plastic (PVC) tube with r radius the $0.05 \text{ mol NaOH/dm}^3$ water solution was flowing towards the arrow direction. Potential difference was switched on 1-cathode and 2-anode. Potential difference was measured between the auxiliary electrodes signed 3 in function of liquid laminar flow velocity beside different polarization potentials (Figure 6).

Figure 6 represents experimental data by porous nickel electrode. According to the results the measured zeta potential values increased quickly beside low flow velocity and low 1000 mV and 2000 mV polarization potentials. The conclusion was, that significant amount of ions broke away. Nevertheless applying 2400 mV polarization potential function of zeta potential versus flow velocity became linear. Then stably attached diffusion layer came into being, which was more difficult to break away. In case of other experiments in less than 2400 mV range, and over 25 cm s^{-1} linear velocity value ζ potential did not change significantly. In that given system it made no sense to apply higher relative velocity.

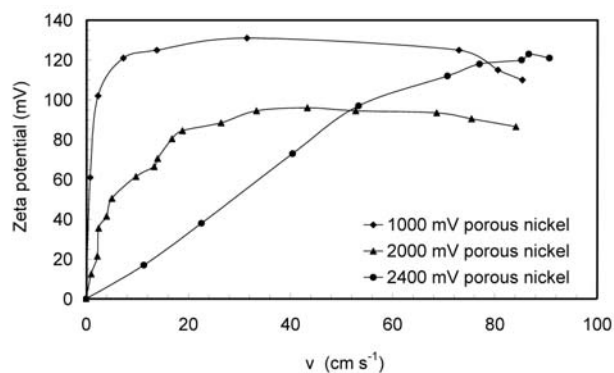


Figure 6. Zeta potential in function of liquid relative flow velocity in case of porous nickel electrodes

Figure 7 represents experimental data by nickelized nickel electrodes. Previous data being compared with results of porous nickel electrodes shows that even at low flow velocities significant amounts of ions break away independently from polarization potential. Hence in nickelized nickel electrodes containing system it makes no sense to apply relative velocity higher than 10 cm s^{-1} .

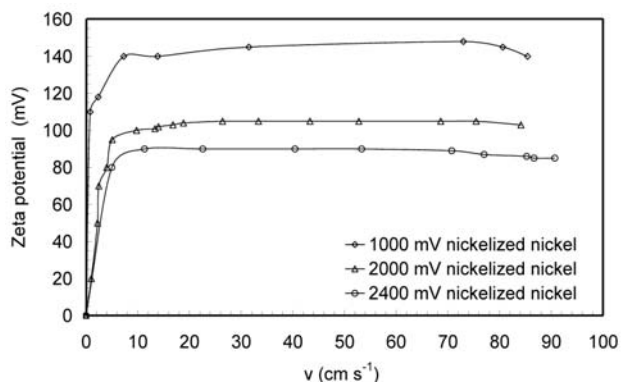


Figure 7. Zeta potential in function of liquid relative flow velocity in case of nickelized nickel electrodes

3. 4. Influence of Physical Adsorption and Adhesive Hydrodynamic Layer

Physical adsorption is superponated on electro-sorption, and adhesive hydrodynamic layer itself took place in ion transport. We measured the relative value of the three processes using $0.05 \text{ mol NaOH/dm}^3$ water solution.

Experiments were carried out as follows: electrodes were dipped into the solution without auxiliary polarization potential, and then physical adsorption of sodium ions took place. Desorption took place in ion exchanged water. After that potential difference switched on the examined electrode (working electrode was always negative, cathode) and graphite counter electrode (positive, anode), so adsorption process was started. Desorption was also taken place in ion exchanged water, meanwhile polarity, electric poles were reversed. We assumed that the electro-sorption and physical adsorption took place simultaneously. Amount of sodium ions taken up by electro-sorption was the mass difference of the two measurements (carried out with and without auxiliary polarization potentials). Results could be compared with calculated data from electric double layer capacity.

Influence of the hydrodynamic adhesive layer: the hydrodynamic adhesive layer moving with electrode could carry ions with itself even if ion adsorption did not exist. Sodium ion concentration would be the same in this case in the hydrodynamic adhesive layer as in the bulk solution.

Adhesive hydrodynamic layer volume was determined for ion exchanged water, and with the help of solution concentration the sodium ion mass transferred by adhesive hydrodynamic layer was calculated ($\text{mg Na}^+ \text{ ion}/(1 \text{ m}^2 \text{ working electrode geometric surface})$).

Figure 8 represents the comparison of the three processes for nickelized nickel-, and porous nickel electrodes and three polarization potentials (1200 mV, 1800 mV, 2400 mV).

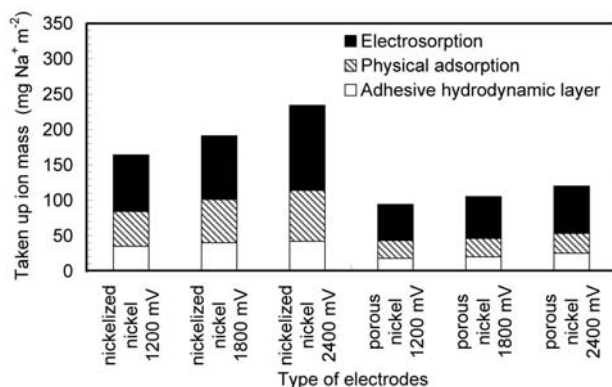


Figure 8. Mass of taken-up ions versus polarization potential in case of nickelized nickel and porous nickel electrodes

We determined that influence of adhesive hydrodynamic layer was significantly lower than adsorption. Mass of adhesive hydrodynamic layer with the increase of potential difference between electrodes did not change, mass of taken up ions with physical adsorption slightly increased, and the mass of taken up ions with electrosorption could be increased applying higher auxiliary polarization potential.

Applying 2400 mV auxiliary polarization potential the measured total mass of taken up Na⁺ ions (adhesive hydrodynamic layer, physical adsorption and electrosorption) related to 1 m² geometrical surface was in case of nickelized nickel electrode 234 mg Na⁺, while for porous nickel electrode it was 120 mg Na⁺. These measured data were approximately the same as the calculated values in the previous (3.2.) chapter. The measured data were used in mathematical model, too.

3. 5. Boundary Layer Separation Method (BLSM)

Obviously ions can be enriched on the properly prepared electrically charged electrode surface compared to the bulk liquid phase. Applying the above phenomena we have developed a new method for the treatment of industrial waste water and named it boundary layer separation method (BLSM). The main point of the method is that the boundary layer at correctly chosen movement velocity can be taken out of the waste water without being damaged, and the ion enriched boundary layer can be recycled.

Electrodes together with boundary layers were cyclically moved between the liquid space vessels being isolated from each other while working electrode was used cyclically as anode or cathode. One cycle contained the next part processes: The large surface nickel working electrodes sank into the solution of the anode-space vessel among the graphite counter electrodes. The proper polarization potential was switched on the constructed electric cell described above so that working electrode was always negative (cathode), while the counter electrode was posi-

ve (anode). Then the positive charged ions were transported to the working electrodes and adsorbed on their surface. That was the so-called electroadsorption phase. Saturation of working electrode could be indicated by the measurement of cell current. After finishing electroadsorption process the ion enriched boundary layer with the working electrode was taken out of the solution (anode-space vessel), and polarization potential was switched off. Then it was placed into the other solution (cathode-space vessel), where polarity, electric pole was reversed. Then the working electrodes changed to positive while counter electrodes in the other cell became negative. As a consequence the electrostatic repulsive force ions desorbed from the surface of working electrodes and transported into the solution. This process could be indicated by the detection of the cell current, too.

In the next step the working electrode was taken out again and the polarization potential was switched off. That was a complete cycle. Applying proper cycle, with boundary layer separation method (BLSM) ion concentration decreased in the anode-space vessel, while ion concentration increased in the cathode-space vessel.

3. 6. Mathematical Model

Oren and Soffer worked out mathematical description for a system, where the solution flows along the non-moving, stationary electrodes.²⁴ According to their theory the boundary layer separation method (BLSM) can also be described. Based on their theory concentrations in anode-space vessel and cathode-space vessel versus cycle number can be calculated. The mathematical model of Oren and Soffer uses mol dm⁻³ concentrations. Let us define the next concentrations:

- $c_A^I(\mathbf{n})$ – anode space (Anode-space) concentration in the n^{th} cycle before electroadsorption at the beginning of the cycle (Initial) (mol dm⁻³)
- $c_A^F(\mathbf{n})$ – anode space (Anode-space) concentration in the n^{th} cycle after electroadsorption at the end of the cycle (Final) (mol dm⁻³)
- $c_C^I(\mathbf{n})$ – cathode space (Cathode-space) concentration in the n^{th} cycle before desorption at the beginning of the cycle (Initial) (mol dm⁻³)
- $c_C^F(\mathbf{n})$ – cathode space (Cathode-space) concentration in the n^{th} cycle after desorption at the end of the cycle (Final) (mol dm⁻³)

Geometrical surface of electrodes is signed G (m²) and the amount of ion mass taken-up by electrodes is m (mol Na⁺ m⁻² geometrical surface). In anode-space vessel and cathode-space vessel the liquid volumes are signed V . If total solution volume in a vessel is V and the ΔV is the volume of adhesive hydrodynamic layer liquid (volume of pores is not included) transferred by electrodes from vessels, then f adhesive hydrodynamic layer liquid ratio remaining on the electrode surface after being taken out of the solution can be calculated as follows:

$$f = \Delta V / V \quad (11)$$

We assume that after electrodes taken-out the concentration of solution in adhesive layer remaining on the surface of the electrodes is the same as the bulk concentration in solution at the end of the cycle. (Our remark is, that m and f values depend on the experimental parameters.)

Ion mass balance for $(n + 1)^{\text{th}}$ cycle in the anode-space vessel:

$$Vc_{A(n+1)}^I = (1-f)Vc_{A(n)}^F + fVc_{C(n)}^F \quad (12)$$

$$Vc_{A(n+1)}^F = Vc_{A(n+1)}^I - mG \quad (13)$$

Ion mass balance for $(n + 1)^{\text{th}}$ cycle in the cathode-space vessel:

$$Vc_{C(n+1)}^I = (1-f)Vc_{C(n)}^F + fVc_{A(n+1)}^F \quad (14)$$

$$Vc_{C(n+1)}^F = Vc_{C(n+1)}^I + mG \quad (15)$$

Concentration difference between cathode-space vessel and anode-space vessel in $(n + 1)^{\text{th}}$ cycle:

$$\Delta c = c_{C(n+1)}^F - c_{A(n+1)}^F \quad (16)$$

With measured taken-up Na^+ ion in mol unit values for nickelized nickel electrodes and porous nickel electrodes calculations were done. Our mathematical calculations were proved by experiments. Using 0.05 mol NaOH/dm^3 water solution cyclic process was carried out with boundary layer separation method (BLSM) by automatic electrosorption equipment. During cyclic process no liquid sample from anode and cathode space vessels were taken to avoid any technical error. According to the above we measured the anodic space vessel and cathodic space vessel Na^+ ion concentrations only after defined cycle numbers (10, 20, 40, 80).

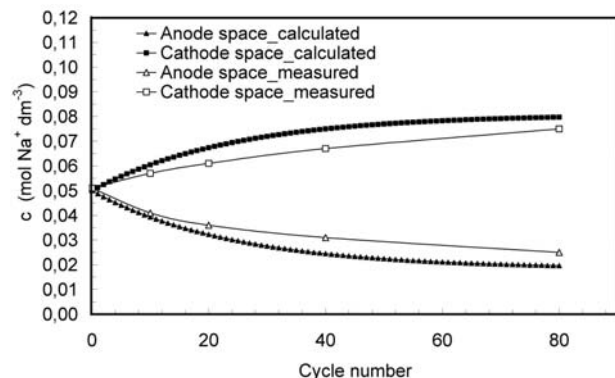


Figure 9. Calculated and measured concentration values in anode space vessel and cathode space vessel versus cycle number in case of nickelized nickel electrode adsorption time 25 s, desorption time 25 s

Comparison of calculated and measured results in case of nickelized nickel electrodes are shown on Figure 9.

For case of nickelized nickel electrode model parameters were $f = 0.0205$ and $m = 234$ ($\text{mg Na}^+ \text{m}^{-2}$ geometrical surface) = 0.01 ($\text{mol Na}^+ \text{m}^{-2}$ geometrical surface).

Measured concentration data agree well with concentration data calculated by mathematical model. Comparisons of calculated and measured data for porous nickel electrodes are shown in Figure 10 and Figure 11. Model parameters are: $f = 0.0098$ and $m = 120$ ($\text{mg Na}^+ \text{m}^{-2}$ geometrical surface) = 0.0052 ($\text{mol Na}^+ \text{m}^{-2}$ geometrical surface).

The conclusion was that m , the taken-up amount of Na^+ ions and f , the liquid ratio was lower than in case of nickelized nickel electrode. In spite of that using the same conditions as for nickelized nickel electrode experiments it was resulted, that in anode space vessel the ion concentration decreased, but in cathode space vessel it was constant. The cause of it was that Na^+ transported into the macro-, meso-, micro pores of the electrode with diffusion and by electric forces. During the applied adsorption, de-

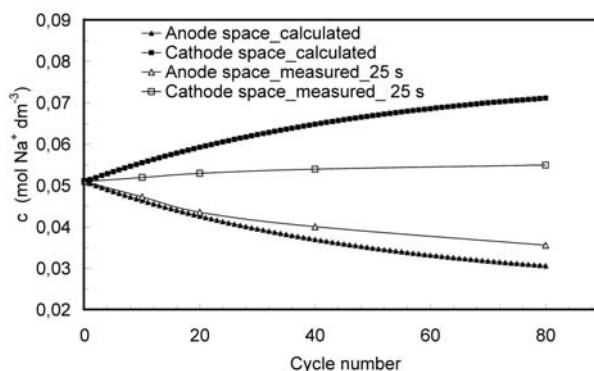


Figure 10. Calculated and measured concentration values ($\text{mol Na}^+/\text{dm}^3$ liquid) in anode space vessel and cathode space vessel versus cycle number in case of porous nickel electrode adsorption time 25 s, desorption time 25 s

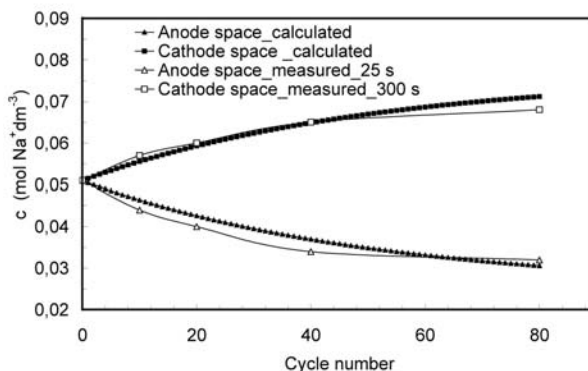


Figure 11. Calculated and measured concentration values in anode space vessel and cathode space vessel versus cycle number in case of porous nickel electrode adsorption time 25 s, desorption time 300 s

sorption process times (25 s) in cathode space vessel in desorption part period Na^+ ions could not get through the boundary layer on electrode to the solution because of hindered pore diffusion. On the other hand in anode space vessel electrode could take up Na^+ ions during the adsorption time to saturate macro-, meso-, micro pores.

When longer adsorption-, desorption process time (300 s) was applied in desorption part period, then ions were able to transport with diffusion into the bulk solution. In this case we got anode space vessel and cathode space vessel measured and calculated concentrations versus cycle number curves shown in Figure 11.

4. Conclusion

We have developed a new method for the treatment of industrial waste water and named it boundary layer separation method (BLSM). The phenomena of ion enrichment in the boundary layer of the electrically charged electrode surface compared to the bulk liquid phase have been applied.

The electrodes were taken out of the waste water with correctly chosen movement velocity to keep the ion enriched boundary layer on the electrode surface. Placing the electrode with boundary layer to another liquid phase the separation could be realized. Nickelized nickel electrodes were produced by electrolysis and powder metallurgical method.

We determined that the electrochemically active surface of nickelized nickel electrodes was larger than that of the porous nickel electrodes. With measurement of Zeta potential could prove that in case of relative movement of electrode and solution the diffuse part breakaway of the electrochemical double layer took place influencing separation effectiveness. We concluded that there was no sense to use higher relative velocity between electrode and solution than 25 cm s^{-1} for porous nickel and 10 cm s^{-1} for nickelized nickel electrodes. Applying graphite electrode electrochemical cell parameters were identified. Taken up sodium ion mass by electrosorption from NaOH water solution could be calculated from the capacity value of electrolytic double layer by means of Faraday law. Related to 1 m^2 electrode geometrical surface for of nickelized nickel electrode the taken up sodium mass was 298 mg Na^+ , while for porous nickel electrode it was 127 mg Na^+ .

We determined with independent measurements the influence of electrosorption, physical adsorption and adhesive hydrodynamic layer on ion transport. Based on the measurements total taken up mass of ions related to 1 m^2 electrode geometrical surface in case of nickelized nickel electrode was 234 mg Na^+ , while for porous nickel electrode it was 120 mg Na^+ .

We discovered that all the three phenomena took place in ion transport. The influence of adhesive hydrodynamic layer was significantly lower than that of adsorp-

tion. Increasing potential difference between electrodes the taken up ion mass by electrosorption could be increased. Based on Oren's and Soffer's publication mathematical description was worked out to calculate concentrations in anode space vessel and cathode space vessel in function of cycle number. Experimental data were compared by the concentration values calculated by the mathematical model. We concluded that application of proper parameters in mathematical model resulted good agreement between measured and calculated concentration values.

Our invented boundary layer separation method named BLSM is a novelty and we have announced patent application at the Hungarian Patent Office³⁴.

5. Acknowledgements

The authors express their gratitude to Chemical Engineering Institute Cooperative Research Centre of the University of Pannonia for financial support of this research study.

6. List of Symbols

$c_A^I(n)$	anode space (Anode-space) concentration in the n^{th} cycle before electroadsorption at the beginning of the cycle (Initial); mol dm^{-3}
$c_A^F(n)$	anode space (Anode-space) concentration in the n^{th} cycle after electroadsorption at the end of the cycle (Final); mol dm^{-3}
$c_C^I(n)$	cathode space (Cathode-space) concentration in the n^{th} cycle before desorption at the beginning of the cycle (Initial); mol dm^{-3}
$c_C^F(n)$	cathode space (Cathode-space) concentration in the n^{th} cycle after desorption at the end of the cycle (Final); mol dm^{-3}
d	distance between conductors (insulator thickness); m
f	adhesive hydrodynamic layer liquid ratio $f = \Delta V / V$
l	distance of auxiliary electrodes; m
m	taken up ions mass on electrodes; mol ion/m^2 geometrical surface of electrodes
t	time; s
v	relative flow velocity; m s^{-1}
r	radius in zeta potential measurement; m
x	cathode-anode distance in case of zeta potential measurement; m
A	capacitor surface; m^2
C_t	polarization capacity at t time; F
C_d	double layer capacity; F
D	diameter; m
G	geometrical surface of electrodes; m^2
I	electric current density; A
Q	electric charge; C
R_e	resistance of electrolyte solution; Ω
R_t	electric charge transfer resistance; Ω
U	potential difference of electric cell; V
V	liquid volume of the anode-, or cathode space vessel; m^3

ΔV	volume of adhesive hydrodynamic layer liquid (volume of pores is not included) transferred by electrodes of vessels; m^3
ϵ	capacitor potential; V
ϵ_0	vacuum permittivity; $F m^{-1}$
ζ	zeta potential; V

7. References

1. C. Rong, H. Xien, *J. Colloid and Interface Science* **2005**, *290*, 190–195.
2. J. Niu, B. E. Conway, *J. Electroanal. Chem.* **2002**, *521*, 16–28.
3. J. Niu, B. E. Conway, *J. Electroanal. Chem.* **2002**, *536*, 83–92.
4. A. Vaškelis, E. Norkus, J. Stalnionienė, G. Stalnionis, *Electrochim. Acta* **2004**, *49*, 1613–1621.
5. A. Afkhauni, B. E. Conway, *J. Colloid and Interface Science* **2002**, *251*, 248–245.
6. Y. Xu, J. W. Zondlo, H. O. Finklea, A. Brennstener, *Fuel Process. Technol.* **2000**, *68*, 189–208.
7. J. C. Farmer, D. V. Fix, G. V. Mack, R. W. Pekala, J. F. Poco, *J. Electrochem. Soc.* **1996**, *143*, 159–169.
8. E. Ayranci, B. E. Conway, *Anal. Chem.* **2001**, *73*, 1181–1189.
9. J. Niu, B. E. Conway, *J. Electroanal. Chem.* **2004**, *564*, 53–63.
10. E. Ayranci, B. E. Conway, *J. Electroanal. Chem.* **2001**, *513*, 100–110.
11. A. Alfarrá, E. Frackowiak, F. Béguin, *Electrochim. Acta* **2002**, *47*, 1545–1553.
12. T. Y. Ying, K. L. Yang, S. Yiacoumi, C. Tsouris, *J. Colloid and Interface Science* **2002**, *250*, 18–27.
13. A. Bán, A. Schäfer, H. Wendt, *J. Appl. Electrochemistry* **1998**, *28*, 227–236.
14. J. Koresh, A. Soffer, *J. Electrochem. Soc.*, **1977**, *124*, 1379–1385.
15. H. Yan, C. F. Blanford, B. T. Holland, M. Parent, W. H. Smyrl, A. Stein, *Adv. Mater* **1999**, *11*, 1003–1006.
16. P. Jiang, J. Cizeron, J. F. Bertone, V. L. Colvin, *J. Am. Chem. Soc.* **1999**, *121*, 7957–7958.
17. S. J. Berezina, G. S. Vozdvizsenszkij, G. P. Deziderev, Dokl. Akad. Nauk SSSR, **1951**, *77*, 53.
18. G. Horányi, E. M. Rizmayer, *J. Electroanal. Chem.* **1984**, *180*, 97–108.
19. V. Ganesh, V. Lakshminarayanan, *Electrochim. Acta* **2004**, *49*, 3561–3572.
20. J. D. Genders, D. Chai, D. T. Hobbs, *J. Appl. Electrochem.* **2000**, *30*, 13–19.
21. D. Hall, Z. Priel, Y. Oren, A. Soffer, *Separation Sci. and Technol.* **1987**, *22*, 1017–1027.
22. Y. Oren, A. Soffer, *J. Appl. Electrochem.* **1983**, *13*, 473–487.
23. Y. Oren, A. Soffer, *J. Appl. Electrochem.* **1983**, *13*, 489–505.
24. Y. Oren, A. Soffer, *J. Electrochem. Soc.* **1978**, *125*, 869–875.
25. Y. Oren, Y. Egozy, *Desalination* **1992**, *86*, 155–172.
26. A. J. Ginffrida, A. D. Jha, G. C. Ganzi, US Patent Num. 4632745, **1986**
27. A. J. Ginffrida, G. C. Ganzi, Y. Oren, US Patent Num. 4956071, **1990**
28. Y. Oren, A. J. Ginffrida, S. Ciaccio, US Patent Num. 5154809, **1992**
29. A. M. Johnson, J. Newman, *J. Electrochem. Soc.* **1971**, *118*, 510–517.
30. E. Norkus, A. Vaškelis, J. Stalnionienė, *J. Solid State Electrochem* **2000**, *4*, 337–341.
31. L. Pan, X. Wang, Y. Gao, Y. Zhang, Y. Chen, S. Zhuo, *Desalination* **2009**, *244*, 139–143
32. E. Bayram, N. Hoda, E. Ayranci, *J. Hazard. Mater.* **2009**, *168*, 1459–1466
33. J. Niu, W. G. Pell, B. E. Conway, *J. Power Sources.* **2006**, *156*, 725–740
34. Hungarian Patent Office, **2009**, Patent Application Num. P0900569

Povzetek

V delu je opisana nova metoda za ravnanje z odpadnimi industrijskimi vodami, imenovana metoda separacije mejne plasti (»boundary layer separation method« -BLSM). Uporabili smo dejstvo, da se ioni zbirajo v mejni plasti tik ob površini elektrode, ki je pod napetostjo. To plast lahko ob primernih pogojih odstranimo iz raztopine in s tem odpadno vodo očistimo. V tem delu smo uporabili dve nikljevi elektrodi z veliko elektroaktivno površino. Najprej smo preverili obstoj difuzijske dvoplasti tik ob elektrodi ter določili njeno kapaciteto. Nato smo uporabili metodo separacije mejne plasti s transportom ionov. Ocenili smo tudi delež adsorpcije ter elektrosorpcije.